

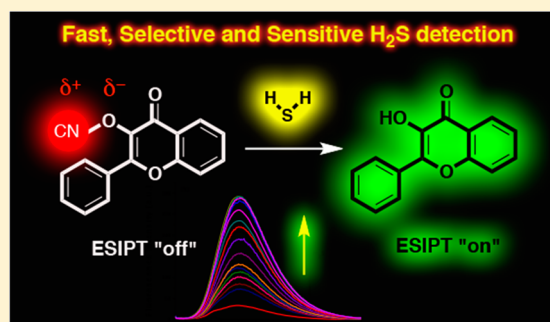
Electrophilic Cyanate As a Recognition Motif for Reactive Sulfur Species: Selective Fluorescence Detection of H₂S

Erman Karakuş, Muhammed Üçüncü, and Mustafa Emrullahoğlu*

Department of Chemistry, Faculty of Science, İzmir Institute of Technology, Urla, 35430, İzmir, Turkey

S Supporting Information

ABSTRACT: An ESIPT-based fluorescent dye, 3-hydroxyflavone, is chemically masked with an electrophilic cyanate motif in order to construct a fluorescent probe for cellular sulfur species. This novel probe structure, displays an extremely fast, highly sensitive and selective “turn-on” type fluorescent response toward H₂S. We have also documented its utility for imaging of H₂S in the living cells.



Hydrogen sulfide (H₂S), the smallest member among cellular sulfur species, plays critical roles in the functioning of living organisms. The compound is produced in biological systems from various sulfur-containing biomolecules and through a range of particular enzymatic pathways.¹ Similar to nitric oxide (NO) and hydrogen peroxide (H₂O₂), H₂S serves as an important gaseous signaling molecule in the nervous, inflammatory, and cardiovascular systems.^{2–5} Cellular H₂S is furthermore involved in an array of physiological events, including the preservation of blood flow and pressure,^{6–8} regulation of cell growth and death,⁹ reduction of ischemia reperfusion injury,^{10–12} regulation of inflammation,¹³ suppression of oxidative stress^{14,15} and antioxidant effects caused by reactions with free radicals.^{16–18} At the same time, an abnormal level of H₂S is attributable to a range of diseases such as chronic kidney disease,¹⁹ liver cirrhosis,²⁰ and Down's syndrome.^{21,22}

The assessment of H₂S levels in the cellular milieu is clearly vital to investigations of cell function and the early diagnosis of some diseases. Understanding the diverse contributions of H₂S to physiology and pathology therefore first requires the development of efficient methods of visualizing H₂S production and distribution in living systems. In related research, sustained attention has been paid to the development of molecular tools for probing cellular sulfur species.^{23–30} Among known analytical tools; fluorescence-based assays are particularly attractive, for they allow the real-time visualization of target species in cellular milieus. During the last several decades, numerous types of fluorescent H₂S probes have appeared in scientific literature on the topic, most of them involving the use of specific chemical reactions to exploit the reactive and reductive nature of H₂S.^{31–41}

In general, the construction of any reaction-based H₂S probe relies on modifying a fluorescent reporter with a reactive masking moiety, which splits away by interacting with H₂S. To attain high selectivity over other relevant sulfur species, these

masking moieties are necessarily highly specific to H₂S (Figure 1).^{42–48}

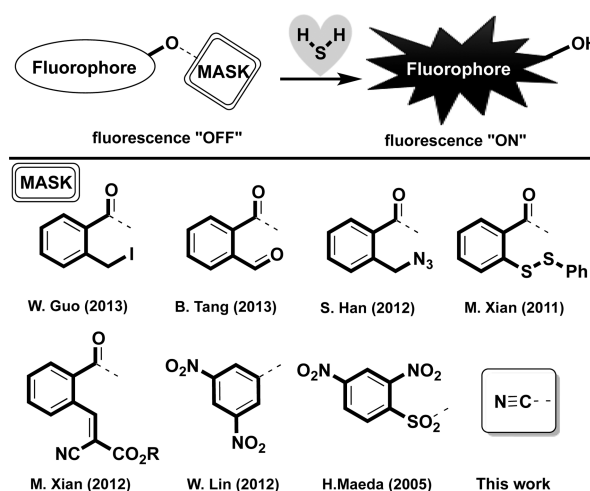


Figure 1. Selected sulfur-sensitive masking groups utilized in fluorescent probe design.

There are several important issues that have to be taken into account when designing a H₂S recognition system. At the heart of the matter lies the discrimination of H₂S over other biological sulfur species such as cysteine and glutathione. Low sensitivity and prolonged response times are other significant stumbling blocks that require attention. Moreover, most masking groups used in probe structures are relatively large

Received: October 28, 2015

Accepted: December 2, 2015

Published: December 2, 2015

organic molecules that have to be prepared individually. In fact, throughout the sensing process, these large masking groups are delivered to the sensing system as organic waste, raising a concern of toxicity. In response, new sensing molecules that use easily accessible and biologically compatible recognition units with improved sensitivity, response times and analyte specificity are needed.

To address these challenges, we have developed a quickly responsive, highly sensitive fluorescent probe for imaging cellular H_2S with excellent selectivity over other potentially competing species. For our probe design, we used an excited-state intramolecular proton transfer (ESIPT)-based fluorescent dye, 3-hydroxyflavone as the signal reporter due to its outstanding photophysical properties, and for the first time in the literature, an electrophilic cyanate (RO-CN) as the H_2S recognition motif.

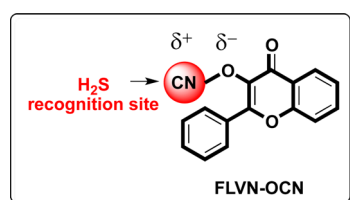


Figure 2. Molecular structure of FLVN-OCN.

EXPERIMENTAL SECTION

General Methods. All reagents were purchased from commercial suppliers (Aldrich and Merck) and used without further purification. ^1H NMR and ^{13}C NMR were measured on a Varian VNMRJ 400 nuclear magnetic resonance spectrometer. UV absorption spectra were obtained on Shimadzu UV-2550 Spectrophotometer. Fluorescence emission spectra were obtained using Varian Cary Eclipse Fluorescence spectrophotometer. Cell imaging was performed with Zeiss Axio fluorescence microscope. Samples were contained in 10.0 mm path length quartz cuvettes (2.0 mL volume). Upon excitation at 415 nm, the emission spectra were integrated over the range 435 to 700 nm (Both excitation and emission slit width 10 nm/10 nm). pH was recorded by HI-8014 instrument (HANNA). All measurements were conducted at least in triplicate.

Synthesis of 3-(cyanooxy)-hydroxyflavone (FLVN-OCN). Compounds **1** and 3-hydroxyflavone were prepared according to literature procedures.⁴⁹ A solution of cyanogen bromide (130 μL , 0.4 mmol) in anhydrous tetrahydrofuran (1 mL) was cooled to -10°C (dry ice/acetone bath). Then, a solution of 3-hydroxyflavone (**1**) (104 mg, 0.4 mol) and triethylamine (58 μL , 0.4 mmol) in anhydrous tetrahydrofuran (1 mL) was added dropwise with magnetic stirring under argon atmosphere. A white precipitate of triethylammonium bromide salt was observed. The mixture was allowed to stir for 1 h. The solution was separated from the salt by filtration and concentrated in vacuo and purified by column chromatography (Hexane:EtOAc 4:1) to afford the compound FLVN-OCN as a white solid. (% 80 isolated yield). ^1H NMR (400 MHz, CDCl_3) δ : 8.11 (d, $J = 8.4$, 1H), 8.04 (d, $J = 6.8$, 1H), 7.91–7.90 (m, 1H), 7.64–7.56 (m, 1H), 7.50–7.42 (m, 4H), 7.34–7.28 (m, 1H). ^{13}C NMR (100 MHz, CDCl_3) δ : 172.0, 157.5, 156.5, 155.5, 154.8, 134.3, 134.0, 131.8, 128.9, 128.6, 125.8, 125.4,

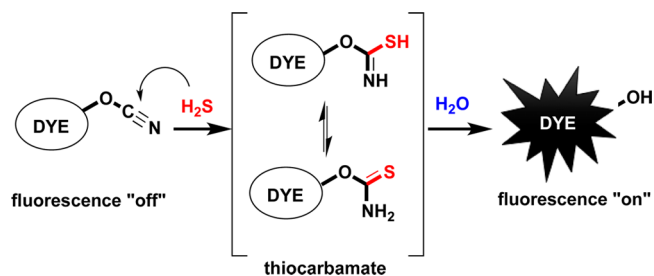
125.0, 123.5, 118.1. Anal. calcd. for $\text{C}_{16}\text{H}_9\text{NO}_3$: C, 73.0; H, 3.45; N, 5.32 found; C, 72.5; H, 3.06; N, 5.03.

Cell Imaging. Human A549 lung adenocarcinoma cell lines were grown in DMEM supplemented with 10% FBS (fetal bovine serum) in an atmosphere of 5% CO_2 at 37°C . The cells were plated on 12 mm cover glasses in 6 well plate and allowed to grow for 24 h. Before the experiments, the cells were washed with PBS buffer, and then cells were treated with 2 mM *N*-methylmaleimide (NMM). After 30 min of NMM-treatment at 37°C , cells were washed with PBS three times. Then FLVN-OCN (10 μM) was added and incubated for 30 min at 37°C then washed with PBS three times. After incubating with Na_2S (50 μM) and CTAB (3 mM) for 30 min at 37°C , cells were rinsed with PBS three times, and DAPI was added and incubated for 10 min at 37°C then washed with PBS three times. The fluorescence images were acquired through fluorescence microscope.

RESULT AND DISCUSSION

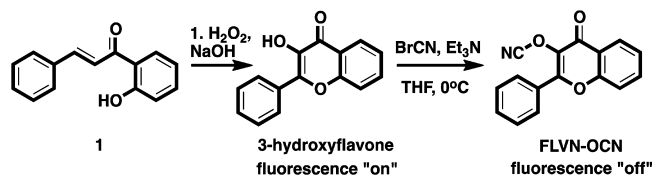
A cyanate (RO-CN) can be used as a reactive nitrile readily added to sulfur species with the formation of thiocarbamates that in aqueous environments rapidly hydrolyses to its hydroxyl derivative. We anticipated that the oxygen-nitrile bond of the prefluorescent dye would undergo selective cleavage in the presence of reactive sulfur species (RSS) and thereby deliver the free hydroxyl derivative of the dye (Scheme 1), which would in turn induce a turn-on type fluorescence response.

Scheme 1. Proposed Mechanism for the Detection of H_2S



The procedure followed to prepare the probe is outlined in Scheme 2. In a single synthetic step, 3-hydroxyflavone was

Scheme 2. Synthesis of FLVN-OCN



treated with commercially available cyanogen bromide in the presence of Et_3N to form the title compound, FLVN-OCN, in a good yield. FLVN-OCN remained quite stable throughout the purification process, and its identity was confirmed by NMR and elemental analysis (see Supporting Information for more details).

The spectroscopic behavior of FLVN-OCN in response to the addition of a range of reactive sulfur species together with other biologically relevant metal and ionic species was investigated by using ultraviolet (UV)-visible and fluorescence spectroscopy in an aqueous solution at pH 7.4. We commenced

our investigation by screening the responses of the probe to a series of RSS, including cysteine, homocysteine, glutathione, and H₂S. As typical of most ESIPT-based turn-on molecular sensors, the masked form of the dye was silent in terms of fluorescence emission. Specifically, FLVN-OCN exhibited no emission in the visible region.

However, with Na₂S or NaHS as the sources, the addition of H₂S to the solution of the probe immediately induced the cleavage of the masking group and concomitantly triggered the formation of the free hydroxyl group, thereby prompting the probe's "off-on" type of spectroscopic response. In the fluorescence spectrum, a new emission band appeared at 525 nm due to a characteristic ESIPT-modulated fluorescence response. At the same time, H₂S could easily be monitored by the naked eye due to its distinct color as well as under the UV lamp due to its changed emission of solution. To our delight, FLVN-OCN showed exceptional selectivity toward H₂S, for no significant changes were monitored in the presence of other competing biothiols such as cysteine, homocysteine, and glutathione.

With the systematic addition of H₂S to FLVN-OCN, the emission band at 525 nm increased linearly over a wide concentration range of H₂S (Figure 3b). Meanwhile, the addition of H₂S prompted the appearance of a new absorption band at 425 nm, with a concomitant decrease in the band at

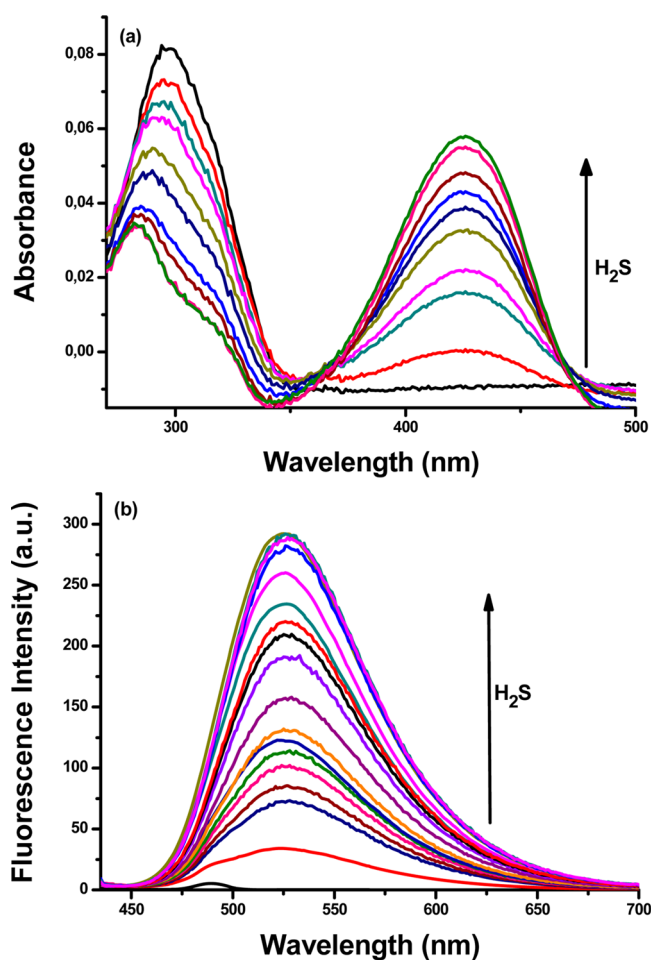


Figure 3. (a) Absorption titration curve of FLVN-OCN (10 μM) and H₂S (0–10 equiv) at pH 7.4. (b) Emission titration curve of FLVN-OCN (10 μM) and H₂S (0 to 10 equiv) at pH 7.4.

297 nm. Under well-established sensing conditions (pH 7.4, cetrimonium bromide (CTAB) 3 mM), we evaluated the detection limit to be 0.25 μM based on $S/N = 3$ (Figure S9). The use of CTAB, in agreement with other reports^{35,40} showed a dramatic contribution to the sensitivity of the sensing system (Figure S8). Notably, under these conditions the response of FLVN-OCN to H₂S at varying concentrations was exceptionally fast (<1 min), and the signal intensity reached its maximum in about 5 min for varying equivalents of H₂S, which marks one of the fastest reaction-based probes developed for H₂S (Figure S2).

In addition, we investigated the possible effects of pH fluctuations in the detection of H₂S. Remarkably, FLVN-OCN showed exceptional stability over a wide pH range (pH 2–9) while remaining nonemissive over the same range. Even in acidic and basic environments, there were no indications of any decomposition of the probe structure. Meanwhile, the response of FLVN-OCN to the addition of H₂S also remained insensitive to changes in the pH. We have also inspected the impact of the added analytes on changing the pH of the sensing media. Systematic control of the solution pH, before and after the incubation of H₂S, proved that the pH of sensing environment remains constant at pH 7.4. Consequently, FLVN-OCN operates efficiently toward H₂S over a wide pH range (pH 4–9), especially under physiological conditions, which is of course imperative for imaging studies of living cells (Figure S7).

To further establish the selectivity of FLVN-OCN, we screened a host of other potentially competing species for their biological significance. As Figure 4 shows, we detected no changes in fluorescence emission in the presence of an excess of other reactive species such as H₂O₂ and HOCl and natural amino acids lacking sulfur functionality, including alanine, arginine, histidine, lysine, methionine, and proline. Moreover, other counterions such as F⁻, Cl⁻, CN⁻, SCN⁻, S₂O₃²⁻, S₂O₅²⁻, PO₄²⁻, and SO₄²⁻, as well as some metal species, including Pd²⁺, Hg²⁺, Cu⁺, Ag⁺, Zn²⁺, and Fe³⁺ induced no distinct spectral changes. All of these findings indicate the exceptional selectivity of FLVN-OCN to H₂S.

We also examined the possible interference of other species in the selectivity of FLVN-OCN by treating the probe with H₂S (5 equiv) in the presence of excess biologically relevant analytes (50 equiv). Nevertheless, FLVN-OCN maintained its selectivity toward H₂S without any perturbation in the fluorescence signal, even in the presence of a high concentration of other competing analytes. These results clearly suggest that FLVN-OCN can accurately detect H₂S in the mixtures of other related species (Figure S6).

We propose that the mechanism of detection is analogous to what has been reported in the literature.⁵⁰ Accordingly, H₂S readily adds to the electrophilic carbon atom of aryl cyanate to yield a thiocarbamate derivative that rapidly hydrolyses in the presence of water to its highly emissive hydroxyaryl derivative (Scheme 1). We consider that the rate of addition determines analyte selectivity. As such, with stronger nucleophiles (e.g., H₂S, pK_a = 7.0), addition to the carbon triple bond occurs at a far higher rate than with weaker nucleophiles (e.g., cysteine and glutathione, pK_a = 8.4), which clearly accounts for the probe's exceptional selectivity toward H₂S.

The promising results of sensing H₂S in the solution encouraged us to further assess the feasibility of the probe to detect H₂S in living cells. To this end, human lung adenocarcinoma cells (A-549) were first treated with 2 mM

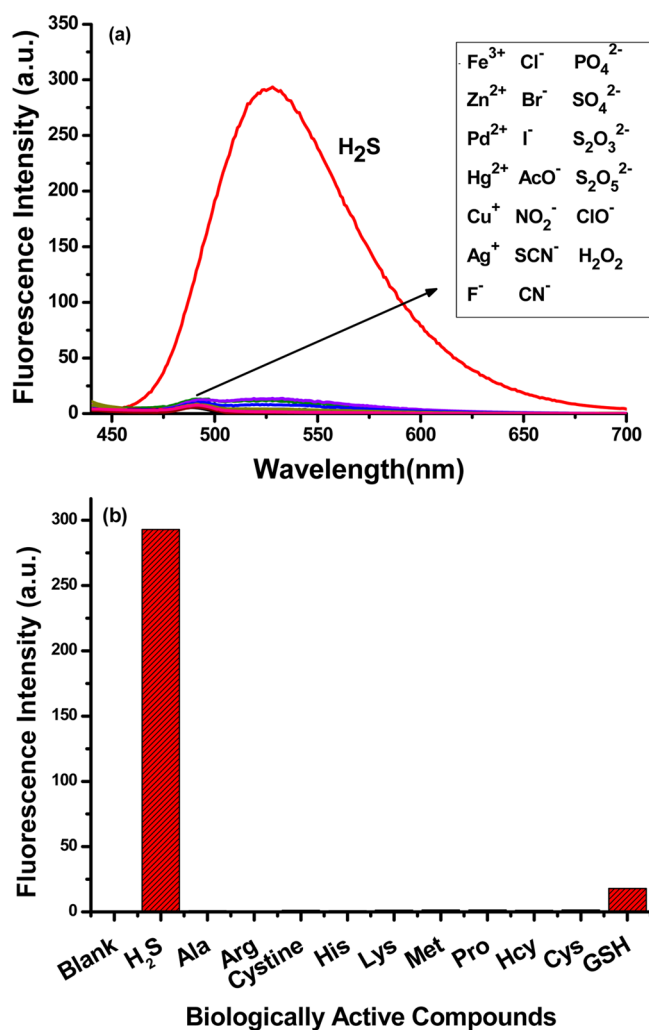


Figure 4. (a) Fluorescence intensities of FLVN-OCN (10 μ M) in an aqueous solution at pH 7.4, emission at 525 nm (λ_{ex} : 415 nm): in the presence of H₂S (5 equiv) and other ions/cations (50 equiv). (b) in the presence of H₂S (5 equiv) and biologically active compounds (50 equiv).

N-methylmaleimide (NMM), a sulfur-trapping agent, to eliminate physiological sulfur species from the cell. The cells were then incubated with FLVN-OCN (10 μ M) for 30 min, to which were added Na₂S (50 μ M) and CTAB (3 mM) and incubated for another 30 min. The cells were stained with a nucleus staining dye (DAPI) for another 10 min, and fluorescence images were taken before and after the addition of Na₂S (50 μ M).

As Figure 5 shows, the human lung adenocarcinoma (A549) cells incubated with FLVN-OCN did not display any fluorescence in the absence of Na₂S species, yet began to emit strongly after incubation with Na₂S. Based on the nucleus counter stain and the characteristic green fluorescence emitting from the cells, we thus conclude that the probe passes through the cell membrane and detects exogenous H₂S from within the cell. The fluorescent microscopy measurement clearly establishes that the probe can be used for imaging H₂S in living cells.

CONCLUSION

In sum, we have developed a fluorescent probe for H₂S by modifying an ESIPT-based fluorescent dye with a cyanate (O-CN) unit as an H₂S-specific recognition motif. The probe

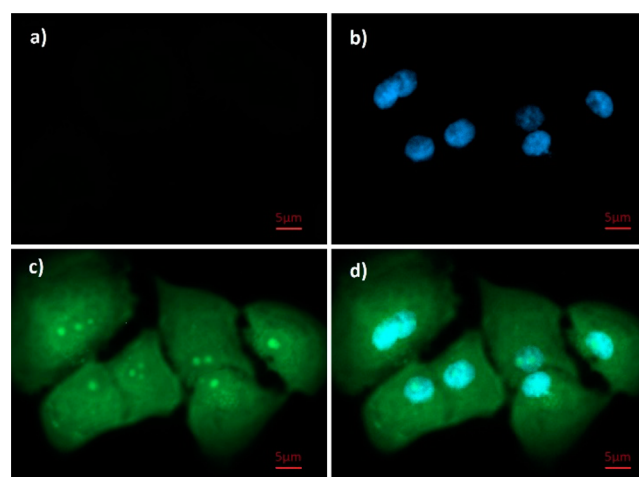


Figure 5. Images of A-549 cells: (a) Cells pretreated with 2 mM NMM for 30 min and then incubated with FLVN-OCN (10 μ M) in the absence of H₂S. (b) cells are detected with DAPI nuclear counterstain (control). (c) cells pretreated with 2 mM NMM then incubated with FLVN-OCN (10 μ M) and H₂S (50 μ M). (d) merged images of frame (b) and (c) DAPI blue, FLVN-OCN green. Scale bar represent 5 μ m.

displayed remarkable fluorescence enhancement (>200 fold), low detection limit (0.25 μ M), and relatively quick response time (<60 s), as well as excellent selectivity toward H₂S over other biological sulfur species such as cysteine, homocysteine and glutathione. In addition, this probe can be used to detect H₂S in both solution and living cells, providing a potentially powerful approach for probing H₂S in biological systems.

ASSOCIATED CONTENT

Supporting Information

The Supporting Information is available free of charge on the ACS Publications website at DOI: 10.1021/acs.analchem.5b04163.

Characterization of FLVN-OCN and all data for UV-vis and fluorescence measurements (PDF)

AUTHOR INFORMATION

Corresponding Author

*E-mail: mustafaemrullahoglu@iyte.edu.tr.

Notes

The authors declare no competing financial interests.

ACKNOWLEDGMENTS

We gratefully acknowledge IZTECH (İzmir Institute of Technology) for financial support and İzmir Institute of Technology, Biotechnology and Bioengineering Research and Application Centre for fluorescence imaging facilities.

REFERENCES

- (1) Kimura, H. *Antioxid. Redox Signaling* **2014**, *20*, 783–793.
- (2) Li, L.; Rose, P.; Moore, P. K. *Annu. Rev. Pharmacol. Toxicol.* **2011**, *51*, 169–187.
- (3) Szabó, C. *Nat. Rev. Drug Discovery* **2007**, *6*, 917–935.
- (4) Lo Faro, M. L.; Fox, B.; Whatmore, J. L.; Winyard, P. G.; Whiteman, M. *Nitric Oxide* **2014**, *41*, 38–47.
- (5) Kolluru, G. K.; Shen, X.; Kevil, C. G. *Redox Biol.* **2013**, *1*, 313–318.

- (6) Köhn, C.; Dubrovskaja, G.; Huang, Y.; Gollasch, M. *Int. J. Biomed. Sci.* **2012**, *8*, 81–86.
- (7) Jackson-Weaver, O.; Osmond, J. M.; Riddle, M.; Naik, J. S.; Gonzalez Bosc, L. V.; Walker, B. R.; Kanagy, N. L. *Am. J. Physiol. Heart Circ. Physiol.* **2013**, *304*, 1446–1454.
- (8) Ariyaratnam, P.; Loubani, M.; Morice, A. H. *Microvasc. Res.* **2013**, *90*, 135–137.
- (9) Yang, G.; Wu, L.; Wang, R. *FASEB J.* **2006**, *20*, 553–555.
- (10) Predmore, B. L.; Lefer, D. J.; Gojon, G. *Antioxid. Redox Signaling* **2012**, *17*, 119–140.
- (11) King, A. L.; Lefer, D. J. *Exp. Physiol.* **2011**, *96*, 840–846.
- (12) Calvert, J. W.; Coetzee, W.; Lefer, D. J. *Antioxid. Redox Signaling* **2010**, *12*, 1203–1217.
- (13) Zanzardo, R. C. O.; Brancalione, V.; Distrutti, E.; Fiorucci, S.; Cirino, G.; Wallace, J. L. *FASEB J.* **2006**, *20*, 2118–2120.
- (14) Kimura, Y.; Goto, Y.-I.; Kimura, H. *Antioxid. Redox Signaling* **2010**, *12*, 1–13.
- (15) Kimura, Y. *FASEB J.* **2004**, 1165–1167.
- (16) Filipovic, M. R.; Miljkovic, J.; Allgäuer, A.; Chaurio, R.; Shubina, T.; Herrmann, M.; Ivanovic-Burmazovic, I. *Biochem. J.* **2012**, *441*, 609–621.
- (17) Jones, C. M.; Lawrence, A.; Wardman, P.; Burkitt, M. J. *Free Radical Biol. Med.* **2002**, *32*, 982–990.
- (18) Carballal, S.; Trujillo, M.; Cuevasanta, E.; Bartesaghi, S.; Möller, M. N.; Folkes, L. K.; García-Bereguiaín, M.; Gutiérrez-Merino, C.; Wardman, P.; Denicola, A. *Free Radical Biol. Med.* **2011**, *50*, 196–205.
- (19) Perna, A. F.; Ingrosso, D. *Nephrol., Dial., Transplant.* **2012**, *27*, 486–493.
- (20) Fiorucci, S.; Antonelli, E.; Mencarelli, A.; Orlandi, S.; Renga, B.; Rizzo, G.; Distrutti, E.; Shah, V.; Morelli, A. *Hepatology* **2005**, *42*, 539–548.
- (21) Han, Y.; Qin, J.; Chang, X.; Yang, Z.; Du, J. *Cell. Mol. Neurobiol.* **2006**, *26*, 101–107.
- (22) Kamoun, P.; Belardinelli, M.-C.; Chabli, A.; Lallouchi, K.; Chadefaux-Vekemans, B. *Am. J. Med. Genet.* **2003**, *116*, 310–311.
- (23) Zhao, Y.; Biggs, T. D.; Xian, M. *Chem. Commun.* **2014**, *50*, 11788–11805.
- (24) Lin, V. S.; Chen, W.; Xian, M.; Chang, C. J. *Chem. Soc. Rev.* **2015**, *44*, 4596–4618.
- (25) Li, J.; Yin, C.; Huo, F. *RSC Adv.* **2015**, *5*, 2191–2206.
- (26) Shimamoto, K.; Hanaoka, K. *Nitric Oxide* **2015**, *46*, 72–79.
- (27) Chen, X.; Zhou, Y.; Peng, X.; Yoon, J. *Chem. Soc. Rev.* **2010**, *39*, 2120–2135.
- (28) Zeng, L.; Chen, S.; Xia, T.; Hu, W.; Li, C.; Liu, Z. *Anal. Chem.* **2015**, *87*, 3004–3010.
- (29) Singha, S.; Kim, D.; Moon, H.; Wang, T.; Kim, K. H.; Shin, Y. H.; Jung, J.; Seo, E.; Lee, S.-J.; Ahn, K. H. *Anal. Chem.* **2015**, *87*, 1188–1195.
- (30) Peng, B.; Zhang, C.; Marutani, E.; Pacheco, A.; Chen, W.; Ichinose, F.; Xian, M. *Org. Lett.* **2015**, *17*, 1541–1544.
- (31) Gupta, N.; Reja, S. I.; Bhalla, V.; Gupta, M.; Kaur, G.; Kumar, M. *Chem. Commun.* **2015**, *51*, 10875–10878.
- (32) Xuan, W.; Pan, R.; Cao, Y.; Liu, K.; Wang, W. *Chem. Commun.* **2012**, *48*, 10669–10671.
- (33) Zhang, H.; Zhang, C.; Liu, R.; Yi, L.; Sun, H. *Chem. Commun.* **2015**, *51*, 2029–2032.
- (34) Zhang, J.; Guo, W. *Chem. Commun.* **2014**, *50*, 4214–4217.
- (35) Liu, Y.; Feng, G. *Org. Biomol. Chem.* **2014**, *12*, 438–445.
- (36) Huang, Z.; Ding, S.; Yu, D.; Huang, F.; Feng, G. *Chem. Commun.* **2014**, *50*, 9185–9187.
- (37) Sasakura, K.; Hanaoka, K.; Shibuya, N.; Mikami, Y.; Kimura, Y.; Komatsu, T.; Ueno, T.; Terai, T.; Kimura, H.; Nagano, T. *J. Am. Chem. Soc.* **2011**, *133*, 18003–18005.
- (38) Peng, B.; Chen, W.; Liu, C.; Rosser, A.; Pacheco, E. W.; Zhao, Y.; Aguilar, H. C.; Xian, M. *Chem. - Eur. J.* **2014**, *20*, 1010–1016.
- (39) Zhao, C.; Zhang, X.; Li, K.; Zhu, S.; Guo, Z.; Zhang, L.; Wang, F.; Fei, Q.; Luo, S.; Shi, P. *J. Am. Chem. Soc.* **2015**, *137*, 8490–8498.
- (40) Tian, H.; Qian, J.; Bai, H.; Sun, Q.; Zhang, L.; Zhang, W. *Anal. Chim. Acta* **2013**, *768*, 136–142.
- (41) Hammers, M. D.; Taormina, M. J.; Cerda, M. M.; Montoya, L. A.; Seidenkranz, D. T.; Parthasarathy, R.; Pluth, M. D. *J. Am. Chem. Soc.* **2015**, *137*, 10216–10223.
- (42) Zhang, J.; Sun, Y.-Q.; Liu, J.; Shi, Y.; Guo, W. *Chem. Commun.* **2013**, *49*, 11305–11307.
- (43) Wang, X.; Sun, J.; Zhang, W.; Ma, X.; Lv, J.; Tang, B. *Chem. Sci.* **2013**, *4*, 2551–2556.
- (44) Wu, Z.; Li, Z.; Yang, L.; Han, J.; Han, S. *Chem. Commun.* **2012**, *48*, 10120–10122.
- (45) Liu, C.; Pan, J.; Li, S.; Zhao, Y.; Wu, L. Y.; Berkman, C. E.; Whorton, R.; Xian, M. *Angew. Chem., Int. Ed.* **2011**, *50*, 10327–10329.
- (46) Liu, C.; Peng, B.; Li, S.; Park, C.-M.; Whorton, R.; Xian, M. *Org. Lett.* **2012**, *14*, 2184–2187.
- (47) Cao, X.; Lin, W.; Zheng, K.; He, L. *Chem. Commun.* **2012**, *48*, 10529.
- (48) Maeda, H.; Matsuno, H.; Ushida, M.; Katayama, K.; Saeki, K.; Itoh, N. *Angew. Chem., Int. Ed.* **2005**, *44*, 2922–2925.
- (49) Liu, X.; Liu, H.; Shen, X.; Song, B.; Bhadury, P. S.; Zhu, H.; Liu, J.; Qi, X. *Bioorg. Med. Chem. Lett.* **2010**, *20*, 4163–4167.
- (50) Jensen, K. A.; Due, M.; Holm, A.; Wentrup, C. *Acta Chem. Scand.* **1966**, *20*, 2091–2106.